

Selective A- or B-site single termination on surfaces of layered oxide SrLaAlO₄

A. Biswas, P. B. Rossen, J. Ravichandran, Y.-H. Chu, Y.-W. Lee, C.-H. Yang, R. Ramesh, and Y. H. Jeong

Citation: *Applied Physics Letters* **102**, 051603 (2013); doi: 10.1063/1.4790575

View online: <http://dx.doi.org/10.1063/1.4790575>

View Table of Contents: <http://scitation.aip.org/content/aip/journal/apl/102/5?ver=pdfcov>

Published by the [AIP Publishing](#)

Articles you may be interested in

Spontaneous B-site order and metallic ferrimagnetism in LaSrVMoO₆ grown by pulsed laser deposition

Appl. Phys. Lett. **102**, 222406 (2013); 10.1063/1.4809937

Layer-by-layer shuttered molecular-beam epitaxial growth of superconducting Sr_{1-x}La_xCuO₂ thin films

J. Appl. Phys. **113**, 053911 (2013); 10.1063/1.4790150

Temperature- and field-dependent critical currents in [(Bi,Pb)₂Sr₂Ca₂Cu₃O_x]_{0.07}(La_{0.7}Sr_{0.3}MnO₃)_{0.03} thick films grown on LaAlO₃ substrates

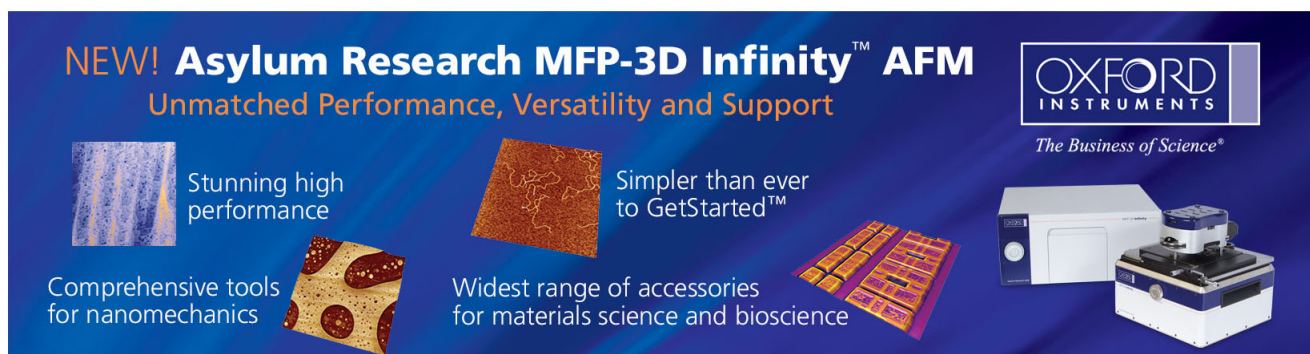
J. Appl. Phys. **113**, 043916 (2013); 10.1063/1.4789348

Preparation and investigation of the A-site and B-site terminated SrTiO₃(001) surface: A combined experimental and theoretical x-ray photoelectron diffraction study

J. Appl. Phys. **112**, 073505 (2012); 10.1063/1.4757283

Atomically flat interface between a single-terminated LaAlO₃ substrate and SrTiO₃ thin film is insulating

AIP Advances **2**, 012147 (2012); 10.1063/1.3688772



NEW! Asylum Research MFP-3D Infinity™ AFM
Unmatched Performance, Versatility and Support

OXFORD INSTRUMENTS
The Business of Science®

Stunning high performance

Simpler than ever to GetStarted™

Comprehensive tools for nanomechanics

Widest range of accessories for materials science and bioscience

(The advertisement includes images of AFM tips, a sample, and the MFP-3D Infinity AFM instrument.)

Selective A- or B-site single termination on surfaces of layered oxide SrLaAlO₄

A. Biswas,^{1,a)} P. B. Rossen,^{2,a)} J. Ravichandran,³ Y.-H. Chu,⁴ Y.-W. Lee,¹ C.-H. Yang,⁵
 R. Ramesh,² and Y. H. Jeong^{1,b)}

¹Department of Physics, Pohang University of Science and Technology, Pohang, 790-784, South Korea

²Department of Materials Science and Engineering, University of California, Berkeley, California 94720, USA

³Applied Science and Technology Graduate Group, University of California, Berkeley, California 94720, USA

⁴Department of Materials Science and Engineering, National Chiao Tung University, Hsin Chu 30013, Taiwan

⁵Department of Physics and Institute for the NanoCentury, KAIST, Daejeon 305-701, South Korea

(Received 6 September 2012; accepted 22 January 2013; published online 4 February 2013)

We demonstrate that thermal annealing in cation controlled environments is an effective means to obtain atomically flat and chemically single terminated surfaces of a layer structured substrate. The effectiveness of the cation controlled annealing method is proved with SrLaAlO₄, which is a representative layer structured substrate of A₂BO₄ type. Potassium ion scattering, in particular, shows that the method allows not only single termination but also selective termination of either A- or B-site on the substrate. We further demonstrate that the chemical nature of underlying SrLaAlO₄ substrates is of critical importance in the growth of SrRuO₃ thin films resulting in different morphologies and transport properties. © 2013 American Institute of Physics.

[<http://dx.doi.org/10.1063/1.4790575>]

Advances in epitaxial growth of oxide thin films, allowing precise control of the interfaces on atomic scale, have led to the discovery of termination dependent interface phenomena such as two dimensional electron gas, superconductivity, and magnetism.^{1,2} An essential prerequisite for high quality oxide epitaxy is, of course, the availability of atomically flat and chemically single terminated substrates.³ Traditional substrate treatments to obtain single terminated surfaces have been limited to ABO₃ type simple perovskites such as SrTiO₃,^{4,5} DyScO₃,⁶ NdGaO₃,⁷ and La_{0.18}Sr_{0.82}Al_{0.59}Ta_{0.41}O₃.⁸ Currently, activities in surface controlled epitaxial growth and interface phenomena of oxide thin films utilize these perovskites, in particular, SrTiO₃. The availability of atomically flat and chemically single terminated substrates of *layered structure*, however, would enrich the study of oxide thin films and heterostructures and allow exploration of new interfacial functionalities. The purpose of the present work is to show that it is indeed possible to obtain an atomically flat surface with single termination on a layered substrate of A₂BO₄ type; we demonstrate that annealing SrLaAlO₄ substrates in proper cation environments is an effective means to create atomically flat surfaces with chemically selective single termination.

SrLaAlO₄ substrates are of great importance as their (001) surface provides a relatively small in-plane lattice constant of 3.7569 Å and thus would be useful in engineering functionality in oxide films with strain effects.^{9,10} SrLaAlO₄ would be of value as an insulating substrate because it maintains insulating nature even under prolonged exposure to reducing conditions. Many substrate materials including SrTiO₃ lose their insulating property when exposed to low oxygen pressures and high temperatures for an extended time.¹¹ SrLaAlO₄ is also useful as a substrate for growing

high T_c superconductors. The superconducting T_c of epitaxial films of La_{1.9}Sr_{0.1}CuO₄ deposited on this substrate reaches 49 K, phenomenally doubling the bulk value of 25 K.¹² For YBa₂Cu₃O_{7-δ} films grown on the same substrate, non-unit cell growth frequently occurs;¹³ it was suspected that this might be related to the chemistry of the substrate surface, but still remains unresolved.

From a structural point of view, SrLaAlO₄ crystallizes in a tetragonal layered K₂NiF₄ structure with lattice constants $a = b = 3.7569 \text{ \AA}$ and $c = 12.6362 \text{ \AA}$ and space group *I4/mmm*.¹⁴ This compound contains AlO₆ octahedra, whereas Sr/La is surrounded only by nine oxygen. The sequence of atomic planes along the c-axis may be represented as –AlO₂–(Sr,La)O–(Sr,La)O–AlO₂–(Sr,La)O–(Sr,La)O– as illustrated in Fig. 1(a); the (Sr,La)O planes are regarded as the A-site layer and the AlO₂ planes as the B-site layer. Despite well known as an oxide substrate with high chemical stability, there have been very few surface studies on this substrate. One report shows that upon annealing in oxidizing conditions, SrO segregates on the surface as particles in combination with holes, creating significant surface roughness.¹⁵ Moreover, the polar nature of the atomic layers and the absence of preferential etchant for (Sr,La)O and AlO₂, make termination control extremely challenging.

The SrLaAlO₄ (001) single crystals (10 × 10 mm²) used in the experiment were commercially available ones provided by CrysTec, GmbH, Germany; the AFM image of the (001) surface of an as-received crystal is shown in Fig. 1(b) (RMS roughness ~1 nm), which presumably has mixed surface termination. Annealing the crystal at 1000 °C for 2 h results in the formation of particles of size 10–50 nm on the surface and particularly on the step edges as displayed in Fig. 1(c). It may be noted that similar particle formation was previously seen in several oxides.^{8,15,16} These particles are soluble in de-ionized water and disappear after soaking for 10 min as Figure 1(d) indicates, and thus they are most likely

^{a)}A. Biswas and P. B. Rossen contributed equally to this work.

^{b)}Author to whom correspondence should be addressed. Electronic mail: yhj@postech.ac.kr.

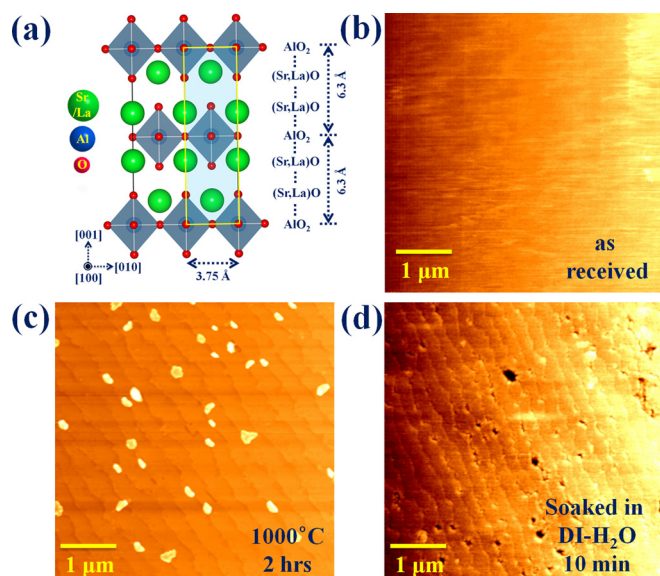


FIG. 1. (a) The crystal structure of SrLaAlO₄ is of tetragonal K₂NiF₄ type having $a = b = 3.75 \text{ \AA}$ and $c = 12.6 \text{ \AA}$. Along c -axis, the layered stacking is $-\text{AlO}_2-(\text{Sr,La})\text{O}-(\text{Sr,La})\text{O}-\text{AlO}_2-(\text{Sr,La})\text{O}-(\text{Sr,La})\text{O}-$, indicated in the yellow rectangular shaded region. (b) The AFM image of the surface of an as-received sample shows roughness of $\sim 1 \text{ nm}$. (c) Thermal annealing at $1000 \text{ }^\circ\text{C}$ for 2 h forms SrO particles of 10–50 nm in size on the surface. (d) These particles are soluble in de-ionized water; after soaking for 10 min, they disappear and nanometer sized holes become visible.

SrO particles because other possible oxide particles such as La₂O₃ and Al₂O₃ are insoluble in water. But this soaking procedure results in increased roughness (RMS roughness $\sim 2 \text{ nm}$), and deteriorates the substrate surface quality.

The formation of SrO particles on the SrLaAlO₄ (001) surface upon annealing suggests the loss of other cations such as La or Al or both from the surface. While the process leading to the SrO formation would be governed by a complex interplay between kinetics and thermodynamics and would be difficult to follow, one may be able to identify experimentally the cations evaporating most from the surface. In Fig. 2(a), the experimental arrangement for this purpose is shown; SrLaAlO₄ (001) substrate is surrounded with La₂O₃ or Al₂O₃ powder as slabs, and thus we provide cation rich annealing environments. It is noted that this cation rich annealing method was previously used for perovskite La_{0.18}Sr_{0.82}Al_{0.59}Ta_{0.41}O₃ substrates, leading to A-site termination only.⁸ After prebaking the powder, the whole setup (substrate + powder) is then annealed. When annealing for 2 h at $1000 \text{ }^\circ\text{C}$ in a La₂O₃ environment, atomically flat surfaces are created without any SrO particles, as evidenced by the AFM images of Figs. 2(b) and 2(c), with a half unit cell step height (0.63 nm) and terrace width $\sim 250 \text{ nm}$. In contrast to the La₂O₃ case, the same thermal treatment with Al₂O₃ in place of La₂O₃ neither prevents the formation of SrO particles nor gives an atomically flat surface. (shown in supplemental material).²¹ Therefore, we conclude that La loss from the surface induces SrO particle formation and La compensation is essential for obtaining atomically flat surfaces.

Having identified La as the key element in achieving structurally well ordered surfaces of SrLaAlO₄, we now turn to another critical issue, that is, the chemical nature of the atomically flat surfaces. At first glance, the half unit cell steps found in the AFM measurements and the layered crystal structure itself naturally suggest that the topmost surface

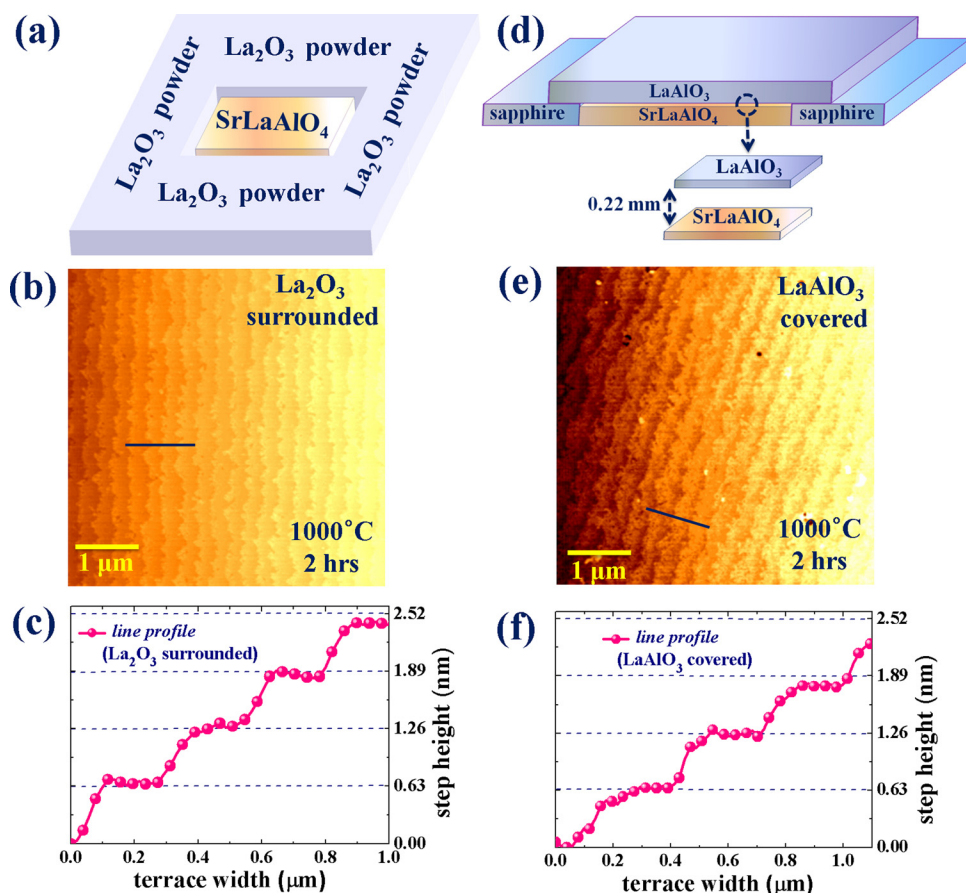


FIG. 2. (a) Annealing setup of a SrLaAlO₄ substrate surface surrounded with La₂O₃ powder. (b) AFM image of the surface after annealing at $1000 \text{ }^\circ\text{C}$ for 2 h reveals terraces and steps. (c) The line profile along the dark line indicated in (b) shows atomically flat step-terrace structure. (d) Annealing setup with LaAlO₃ covered. (e) AFM image of the surface after annealing at $1000 \text{ }^\circ\text{C}$ for 2 h reveals terraces and steps. (f) The line profile along the dark line indicated in (e) shows atomically flat step-terrace structure. The step height corresponds to the half unit cell lattice spacing of 0.63 nm.

layer would be single terminated with (Sr,La)O, i.e., A-site terminated. These considerations, however, may not necessarily exclude a possibility of B-site termination in case Al ions are supplied simultaneously with La ions in the surrounding vapor during the annealing process. To check this possibility, however mere it is, an attempt was made to use a LaAlO₃ crystal as a vapor source. A LaAlO₃ crystal was placed in close proximity to the surface of SrLaAlO₄ (0.22 mm gap between the surfaces) with polished side facing each other as shown in Fig. 2(d); the whole setup is then annealed at 1000 °C for 2 h. Fig. 2(e) is the obtained AFM image after annealing the SrLaAlO₄ (001) surface, and it shows that the surface is atomically flat with the step height of ~0.63 nm and terrace width of ~250 nm as seen in Fig. 2(f). Thus, we have achieved equal structural successes both with La₂O₃ and with LaAlO₃ as background cation sources in the annealing treatments of SrLaAlO₄ (001) substrates. Moreover, these treated substrates (10 × 10 mm², thickness 0.5 mm) were found to remain insulating with resistance larger than 10¹⁰ Ω when exposed to reducing conditions of 900 °C and O₂ pressure of 10⁻⁷ Torr for several hours. The remaining task is to examine and identify the chemical nature of the topmost layers of the thermally treated crystals.

In order to identify the topmost atomic layer, we employed angle resolved mass spectroscopy of recoiled ions (AR-MSRI) analysis along with direct recoil spectroscopy (DRS) to determine the surface termination of as-received and treated substrates. For scattering purposes, pulsed potassium ions (³⁹K) with a kinetic energy of 10 keV are injected on the surface of the substrates at an incident angle of 15°, scattered and recoiled species from the sample are collected at 25° using a multichannel plate detector for DRS and 60° using a reflectron analyzer for MSRI as illustrated in the inset of Fig. 3.¹⁷ All the AR-MSRI and DRS (Ionwerks, Inc.) measurements were conducted in high vacuum (10⁻⁷ Torr) at 150 °C. Prior to the measurements, the substrates were

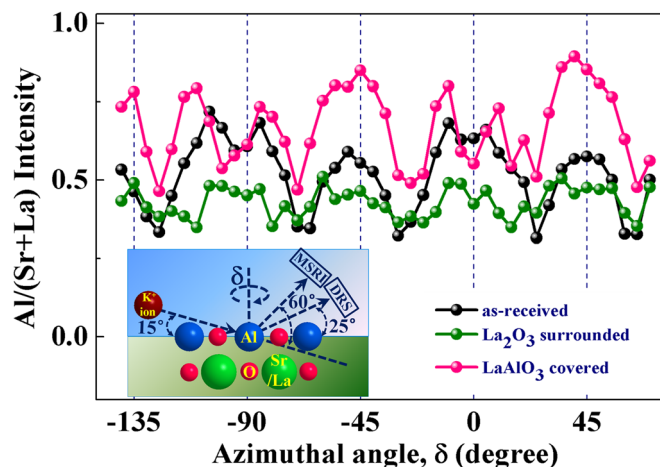


FIG. 3. The ratio of the Al signal against the sum of the Sr and La signals from AR-MSRI is shown for substrates as they were received (black) and that went through annealing processes in La₂O₃ (green) and LaAlO₃ (pink) environments. The decreased (La₂O₃ surrounded) and increased (LaAlO₃ covered) ratios at ±45° are indications for A-site and B-site terminations, respectively. Illustrated in the inset is a schematic for time of flight ion scattering and recoil spectroscopy experiments using pulsed potassium (³⁹K) ions. Detectors for AR-MSRI and DRS are indicated in the figure.

annealed at 600 °C in 50 mTorr of oxygen gas to remove hydrocarbon contaminations. In general, [100] and [010] correspond to ±0° and ±90° of the azimuth and [110] as ±45° and ±135° of the azimuth. The kinetic energy of recoiled atoms is proportional to their mass, allowing a direct conversion from time of flight to atomic mass. The intensities of recoiled ions are naturally influenced by neighboring ions and their arrangements; the variation of recoiled intensities and their ratios as a function of azimuthal angle is commonly used to evidence single terminated surfaces for perovskite oxides, particularly along the [110] direction where the A-site and B-site cations shadow one another.^{6,18} However, it should be kept in mind that SrLaAlO₄ is not an actual perovskite but a layered one. The (Sr,La)O double layer of the system has a [1/2¹/2/0] displacement, which permits blocking and shadowing effects in [100] and [010] directions as well as [110] direction.

In Fig. 3, the Al/(Sr + La) ratio extracted from the AR-MSRI measurements is shown for the three SrLaAlO₄ substrates, as-received one (black circles) and annealed ones in La₂O₃ (green circles) and LaAlO₃ (pink circles) environments. The signal from the as-received sample is regarded as the reference, and the signals from the treated samples are compared with the reference because the as-received sample is expected to have mixed termination. For the La₂O₃ treated sample (green circles), it is seen that there is an overall decrease in the Al/(Sr + La) ratio intensity from the reference values (black circles), and the most severe reductions from the reference occur in the low index crystalline directions such as 0°, ±90°, and ±45° angles, corresponding to [100], [010], and [110] directions, respectively. These features, in particular, the reduction in the [110] direction, indicate (Sr,La)O as the topmost layer of the La₂O₃ treated sample. For the LaAlO₃ treated sample, on the other hand, an overall increase in the Al/(Sr + La) intensity is observed with the exception of 0° and ±90°, [100] and [010] directions, respectively, in Fig. 3. The largest increase is seen at ±45°, or in the [110] direction, and this corresponds to shadowing of (Sr,La) by Al, indicating AlO₂ as the topmost layer. The behaviors at 0° and ±90° suggest that (Sr,La)O is the second layer.

For further insight in the cation arrangements of the top layers, individual cation ratios again extracted from the AR-MSRI measurements are given in Fig. 4. It may be noted that the Al/Sr and Al/La ratios for the as-received substrate show the more or less same variation as a function of azimuthal angle as the Al/(Sr + La) ratio of the same sample, while the Sr/La ratio shows almost no variation. These features indicate that there is a good mixing of Sr and La in the (Sr,La)O layer on the surface. The occurrence of distinctive minima in the Al/Sr ratio of the La₂O₃ treated sample in [110] as well as [010] and [100] directions, as shown in Fig. 4(a), is the evidence of shadowing of Al by two layers of Sr thus confirming (Sr,La)O as top layer. The low intensity peaks for all low index crystalline directions for the Al/La ratio in Fig. 4(b) suggest that there is a negligible amount of La on top of the first AlO₂ layer. The LaAlO₃ treated sample also has increased values for the Al/Sr ratio and a strong maximum for the Al/La ratio in the [110] direction; this indicates shadowing of both La and Sr by Al and therefore evidencing

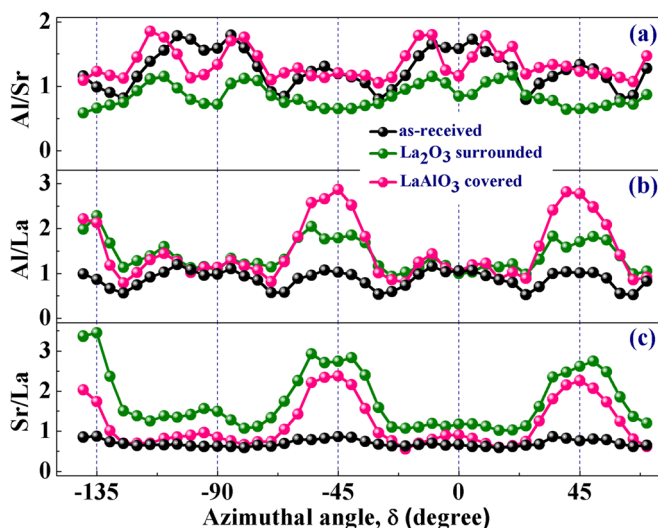


FIG. 4. Individual cation ratios extracted from the AR-MSRI measurements are shown. (a) The ratio between Al and Sr. (b) The ratio between Al and La. (c) The ratio between Sr and La. These data provide further insight in the cation arrangements of the top layers, and reveal La poor layers for annealed substrates.

AlO_2 to be the topmost layer. The minimum in both Al/Sr and Al/La ratios in the [010] direction indicates only a single layer of AlO_2 at the top. Fig. 4(c) shows that strong maxima along the [110] direction exist in the Sr/La ratio for both La_2O_3 treated and LaAlO_3 treated substrates, indicating that the annealing process results generally in somewhat La-poor (Sr,La)O layers at the surface, as compared to the as-received substrate. This shows that despite the presence of La rich environments, high temperature annealing processes invariably create La depleted surfaces.

Additional confirmation of the surface termination can be obtained from the DRS analysis of the scattered potassium ion intensities, $K_s(\text{Sr,La})$ and $K_s(\text{Al})$ scattered from heavy (Sr, La) and light (Al) elements, respectively. (Cationic analysis of the DRS spectra is given in supplemental mate-

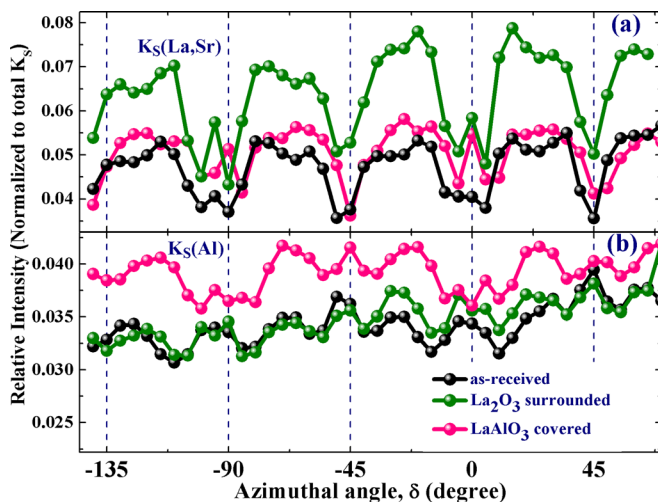


FIG. 5. Relative intensities from the DRS spectra are shown for potassium scattered off (Sr,La) in (a) and off Al in (b), designated as $K_s(\text{Sr,La})$ and $K_s(\text{Al})$, respectively. The $K_s(\text{Sr,La})$ intensity is significantly higher for the La_2O_3 surrounded sample than others, indicating (Sr,La)O termination. The $K_s(\text{Al})$ intensity is significantly higher for the LaAlO_3 covered sample, indicating AlO_2 termination.

rial.)²¹ The analysis shows that there is an overall increase in $K_s(\text{Sr,La})$ for the La_2O_3 treated sample compared to the as-received or LaAlO_3 treated case, indicating (Sr,La)O as the topmost layer as shown in Fig. 5(a). On the other hand, Fig. 5(b) shows contrasting overall increase in the intensity of $K_s(\text{Al})$ for the LaAlO_3 treated sample, indicating AlO_2 as the topmost layer. Thus, judging from the AR-MSRI results with further support from the DRS data, we are led to the (Sr,La)O-(Sr,La)O- AlO_2 layer sequence from the surface, with the La poor topmost layer, for the La_2O_3 treated sample, and to the AlO_2 -(Sr,La)O-(Sr,La)O layer sequence, where the first (Sr,La)O is likely to be La poor, for the LaAlO_3 treated sample.

While we have determined the topmost terminating layer of SrLaAlO_4 substrates by various probing techniques, thin film growth itself may be used as a way to ascertain different terminations. For this purpose, we chose SrRuO_3 as an oxide material to grow on the treated substrates; it was seen earlier that SrRuO_3 tends to grow preferably on B-site terminated surfaces of SrTiO_3 substrates.¹⁹ Thin films of 30 nm were grown at 700 °C with oxygen partial pressure of 10 mTorr and laser pulses at 2 Hz, using a KrF laser ($\lambda=248$ nm). After growth samples were slowly cooled down in oxygen environments. Figs. 6(a) and 6(b) show the morphology of films grown on a (Sr,La)O terminated substrate and an AlO_2 terminated substrate, respectively. Array of large trenches is visible for films grown on (Sr,La)O terminated substrates. It may be noted that deep trenches were previously observed when SrTiO_3 substrates had SrO termination in addition to TiO_2 termination.^{20,21} Contrasting morphologies in the figure clearly exhibit termination dependent

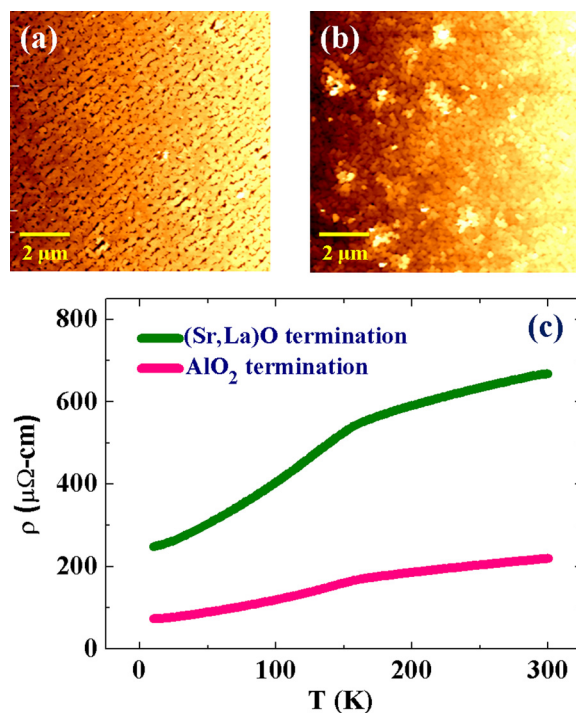


FIG. 6. AFM images of SrRuO_3 films grown on different terminated substrates; (a) (Sr,La)O termination, (b) AlO_2 termination. For the film grown on (Sr,La)O terminated substrate, clear nm sized trenches are visible, which are absent for that on AlO_2 terminated substrate; this selective growth preference of SrRuO_3 confirming different substrate terminations. (c) Resistivity of the two samples showing morphology dependent transport behavior.

growth of SrRuO₃ films. Resistivity measurements also show a strong dependence on growth morphology as is seen in Fig. 6(c). These behaviors indicate that we have selective termination of either (Sr,La)O or AlO₂ on SrLaAlO₄ substrates, and growth of oxide thin films is sensitive to the chemical nature of the top surface. The availability of atomically flat and chemically single terminated substrates beyond simple perovskites would broaden the research horizon for oxide epitaxy and interface phenomena.

In conclusion, the present work demonstrated that annealing a substrate in proper cation environments is an effective means to create atomically flat surfaces with selective termination of A- or B-type in a common substrate such as SrLaAlO₄. The detailed AR-MSRI and DRS measurements were used to confirm that the layer sequences for La₂O₃ and LaAlO₃ treated SrLaAlO₄ substrates are (Sr,La)O-(Sr,La)O-AlO₂ and AlO₂-(Sr,La)O-(Sr,La)O from the surface, respectively. SrRuO₃ films grown on SrLaAlO₄ substrates showed termination dependent morphology and transport behaviors. While the present work provides a pathway for obtaining both A- and B-site terminated atomically flat A₂BO₄ type layered oxide surfaces, our theoretical understanding of the processes occurring during the annealing treatments is limited. Further investigations, experimental as well as theoretical, are clearly needed to generalize the method to more diverse systems. It should be noted that the ability to singly terminate a substrate surface selectively with atomic flatness without depositing a top layer is of critical importance for the advancement of high quality oxide thin films and heterostructures, which in turn would provide a platform for studying the physics of interface phenomena, high T_c superconductors, polar and non-polar surface reconstructions, advanced device applications, etc.

Y.H.J. and C.H.Y. acknowledge the supports by National Research Foundation funded by the Ministry of Education, Sci-

ence and Technology of Korea (2010-0013528, 2011-0018037, 2011-0009231, and SRC 2011-0030046). J.R. acknowledges the Link Foundation.

- ¹A. Ohtomo and H. Hwang, *Nature* **427**, 423 (2004).
- ²L. Li, C. Richter, J. Mannhart, and R. C. Ashoori, *Nature Phys.* **7**, 762 (2011).
- ³D. G. Scholm, L. Q. Chen, X. Pan, A. Schmehl, and M. A. Zurbuchen, *J. Am. Ceram. Soc.* **91**, 2429 (2008).
- ⁴M. Kawasaki, K. Takahashi, T. Maeda, R. Tsuchiya, M. Shinohara, O. Ishiyama, T. Yonezawa, M. Yoshimoto, and H. Koinuma, *Science* **266**, 1540 (1994).
- ⁵R. Bachelet, F. Sanchez, F. J. Palomares, C. Ocal, and J. Fontcuberta, *Appl. Phys. Lett.* **95**, 141915 (2009).
- ⁶J. E. Kleibecker, G. Koster, W. Siemons, D. Dubbink, B. Kuiper, J. L. Blok, C.-H. Yang, J. Ravichandran, R. Ramesh, J. E. ten Elshof, D. H. A. Blank, and G. Rijnders, *Adv. Funct. Mater.* **20**, 3490 (2010).
- ⁷T. Ohnishi, K. Takahashi, M. Nakamura, M. Kawasaki, M. Yoshimoto, and H. Koinuma, *Appl. Phys. Lett.* **74**, 2531 (1999).
- ⁸J. H. Ngai, T. C. Schwendemann, A. E. Walker, Y. Segal, F. J. Walker, E. I. Altman, and C. H. Ahn, *Adv. Mater.* **22**, 2945 (2010).
- ⁹D. G. Schlom, L.-Q. Chen, C.-B. Eom, K. M. Rabe, S. K. Streiffer, and J.-M. Triscone, *Annu. Rev. Mater. Res.* **37**, 589 (2007).
- ¹⁰J. M. Rondinelli and N. A. Spaldin, *Adv. Mater.* **23**, 3363 (2011).
- ¹¹W. Siemons, G. Koster, H. Yamamoto, W. A. Harrison, G. Lucovsky, T. H. Geballe, D. H. A. Blank, and M. R. Beasley, *Phys. Rev. Lett.* **98**, 196802 (2007).
- ¹²J.-P. Locquet, J. Perret, J. Fompeyrine, E. Mächler, J. W. Seo, and G. Van Tendeloo, *Nature* **394**, 453 (1998).
- ¹³T. Haage, Q. D. Jiang, M. Cardona, H. U. Habermeier, and J. Zegenhagen, *Appl. Phys. Lett.* **68**, 2427 (1996).
- ¹⁴X. C. Fan, X. M. Chen, and X. Q. Liu, *Chem. Mater.* **20**, 4092 (2008).
- ¹⁵A. E. Becerra-Toledo and L. D. Marks, *Surf. Sci.* **604**, 1476 (2010).
- ¹⁶K. Szot, W. Speier, U. Breuer, R. Meyer, J. Szade, and R. Waser, *Surf. Sci.* **460**, 112 (2000).
- ¹⁷J. Wayne Rabalais, *Principles and Applications of Ion Scattering Spectrometry* (John Wiley & Sons, Hoboken, 2003).
- ¹⁸A. Biswas, P. B. Rossen, C.-H. Yang, W. Siemons, M.-H. Jung, I. K. Yang, R. Ramesh, and Y. H. Jeong, *Appl. Phys. Lett.* **98**, 051904 (2011).
- ¹⁹G. Rijnders, D. H. A. Blank, J. Choi, and C.-B. Eom, *Appl. Phys. Lett.* **84**, 505 (2004).
- ²⁰R. Bachelet, F. Sánchez, J. Santiso, C. Munuera, C. Ocal, and J. Fontcuberta, *Chem. Mater.* **21**, 2494 (2009).
- ²¹See supplementary material at <http://dx.doi.org/10.1063/1.4790575> for optimized annealing treatments and DRS spectra analysis.